



Citation for published version:

Blenkinsopp, CE, Bayle, PM, Conley, DC, Masselink, G, Gulson, E, Kelly, I, Almar, R, Turner, IL, Baldock, TE, Beuzen, T, McCall, RT, Rijper, H, Reniers, A, Troch, P, Gallach-Sanchez, D, Hunter, AJ, Bryan, O, Hennessey, G, Ganderton, P, Tissier, M, Kudella, M & Schimmels, S 2021, 'High-resolution, large-scale laboratory measurements of a sandy beach and dynamic cobble berm revetment', *Scientific Data*, vol. 8, no. 1, 22. <https://doi.org/10.1038/s41597-021-00805-1>

DOI:

[10.1038/s41597-021-00805-1](https://doi.org/10.1038/s41597-021-00805-1)

Publication date:

2021

Document Version

Peer reviewed version

[Link to publication](#)

University of Bath

Alternative formats

If you require this document in an alternative format, please contact:
openaccess@bath.ac.uk

General rights

Copyright and moral rights for the publications made accessible in the public portal are retained by the authors and/or other copyright owners and it is a condition of accessing publications that users recognise and abide by the legal requirements associated with these rights.

Take down policy

If you believe that this document breaches copyright please contact us providing details, and we will remove access to the work immediately and investigate your claim.

1 **Title**

2 *High-resolution, large-scale laboratory measurements of a sandy beach and dynamic cobble*
3 *berm revetment*

4
5 **Authors**

6 Chris E Blenkinsopp¹, Paul M Bayle¹, Daniel Conley², Gerd Masselink², Emily Gulson², Isabel
7 Kelly², Rafael Almar³, Ian L Turner⁴, Tom E Baldock⁵, Tomas Beuzen^{4,6}, Robert McCall⁷, Huub
8 Rijper^{7,8,9}, Ad Reniers⁹, Peter Troch¹⁰, David Gallach-Sanchez^{10,11}, Alan Hunter¹², Oscar Bryan¹²,
9 Gwyn Hennessey¹, Peter Ganderton², Marion Tissier⁹, Matthias Kudella¹³, Stefan Schimmels¹³

10
11
12 **Affiliations**

13 1. Centre for Infrastructure, Geotechnics and Water Engineering, Department of Architecture
14 and Civil Engineering, University of Bath, Bath BA2 7AY, UK

15 2. School of Biological and Marine Sciences, Plymouth University, Drake Circus, PL4 8AA
16 Plymouth, UK

17 3. IRD-LEGOS, UMR5566, 18 Av. Edouard Belin, 31400 Toulouse, France

18 4. Water Research Laboratory, School of Civil and Environmental Engineering, UNSW Sydney,
19 NSW 2052, Australia

20 5. School of Civil Engineering, University of Queensland, Brisbane, QLD, 4072, Australia

21 6. Department of Statistics, University of British Columbia, Vancouver, Canada

22 7. Department of Marine and Coastal Systems, Deltares, Boussinesqweg 1, 2629 HV Delft,
23 the Netherlands

24 8. Royal Boskalis Westminster N.V., Rosmolenweg 20, 3356 LK Papendrecht, the Netherlands

25 9. Faculty of Civil Engineering and Geosciences, Delft University of Technology, Stevinweg 1,
26 2628 CN Delft, the Netherlands

27 10. DEME Group, Scheldedijk 30, 2070 Zwijndrecht, Belgium

28 11. Department of Civil Engineering, Ghent University, Technologiepark 60, Ghent, B-9052,
29 Belgium

30 12. Department of Mechanical Engineering, University of Bath, Bath BA2 7AY, UK

31 13. Forschungszentrum Küste (FZK), Merkurstraße 11, 30419 Hannover, Germany

32
33 * currently at Department of Statistics, University of British Columbia, Vancouver, Canada

34 ** currently at Royal Boskalis Westminster N.V., Rosmolenweg 20, 3356 LK Papendrecht, the
35 Netherlands

36 *** currently at DEME Group, Scheldedijk 30, 2070 Zwijndrecht, Belgium

37
38 corresponding author(s): Chris Blenkinsopp (c.blenkinsopp@bath.ac.uk)

39
40 **Abstract**

41 High quality laboratory measurements of nearshore waves and morphology change at, or
42 near prototype-scale are essential to support new understanding of coastal processes and
43 enable the development and validation of predictive models. The DynaRev experiment was
44 completed at the GWK large wave flume over 8 weeks during 2017 to investigate the
45 response of a sandy beach to water level rise and varying wave conditions with and without
46 a dynamic cobble berm revetment, as well as the resilience of the revetment itself. A large
47 array of instrumentation was used throughout the experiment to capture: (1) wave
48 transformation from intermediate water depths to the runup limit at high spatio-temporal
49 resolution, (2) beach profile change including wave-by-wave changes in the swash zone, (3)
50 detailed hydro and morphodynamic measurements around a developing and a translating
51 sandbar.

53 **Background & Summary**

54

55 High quality field and numerical investigations are providing new insights into a wide variety
56 of coastal processes and coastal protection solutions^{1,2}. However, numerical modelling
57 approaches are not yet capable of accurately reproducing all coastal hydro and
58 morphodynamic phenomena, and the difficulties involved in capturing field data in the
59 desired wave, tide and wind conditions mean that controlled laboratory wave flume
60 experiments remain extremely valuable. Large-scale experiments^{3,4} are particularly valuable
61 as they mostly avoid scaling issues, and improvements in the instrumentation and
62 measurement techniques available mean that the quality and resolution of data continues to
63 improve and provide new insights.

64

65 The DynaRev experiment was designed to investigate the response of a sand beach and the
66 resilience of a dynamic cobble berm revetment to constant wave forcing and a rising water
67 level at large-scale in a controlled laboratory environment through high spatio-temporal
68 resolution morphology measurements (Figure 1). A dynamic cobble berm revetment is a
69 nature-based coastal protection approach which consists of a cobble ridge constructed
70 around the high tide runup limit to artificially mimic composite beaches⁵. This commonly
71 occurring beach type consists of a lower foreshore of sand and a backshore ridge
72 constructed of gravel or cobbles that stabilises the upper beach and provides overtopping
73 protection. Dynamic revetment structures contrast with static coastal defence structures as
74 they are specifically designed to reshape under wave attack. In addition to the morphology
75 data, high-resolution measurements of nearshore hydrodynamic processes were also
76 collected.

77 DynaRev took place over a 2-month period from August to September 2017 in the 309 m
78 long Large Wave Flume (Großer Wellenkanal, GWK), Hannover, Germany. A total of 141.6
79 hours of testing under wave action was completed. This testing comprised two “phases”,
80 with each phase being split into a series of “runs” varying from 20 minutes to 3 hours in
81 duration. The beach profile was only reset between the two phases, thus all runs had a
82 different antecedent morphology corresponding to the beach profile the end of the
83 preceding run.

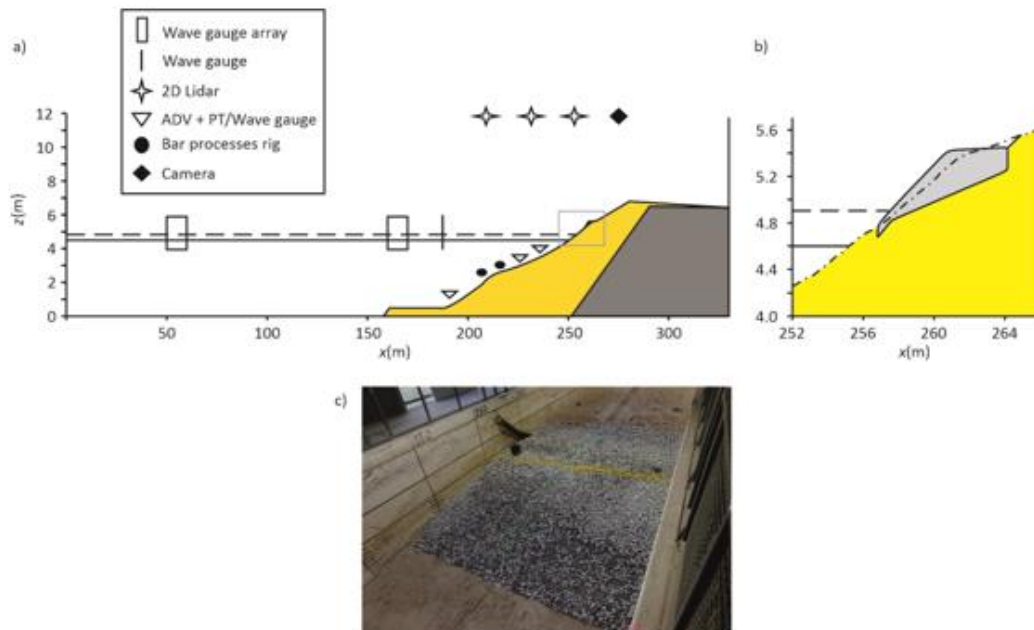
84 *Phase SB - Unmodified sand beach response to a rising water level:* Starting with a plane 1:15
85 sand slope, the evolution of the beach profile was measured under constant wave forcing (H_s
86 = 0.8 m, T_p = 6.0 s) for 20 hours. The mean water level in the flume was then raised from an
87 initial elevation z_{wl} = 4.5 m by a total of 0.4 m in incremental steps of 0.1 m (38 hours of
88 water level rise testing). Following the completion of the water level rise increments, the
89 short-term response of the beach was measured at the final water level (z_{wl} = 4.9 m) for a
90 range of different wave conditions expected to produce both erosion and accretion.

91 *Phase DR - Dynamic cobble berm revetment response to a rising water level:* Again starting
92 with a manually reshaped 1:15 plane slope, a sand beach was measured as it evolved under
93 the same constant wave conditions as used in Phase SB for 20 hours to provide a natural
94 beach profile on which to construct the dynamic revetment. Following this, the same water
95 level increments and test durations as for Phase SB were applied. Prior to the first water
96 level increment, a cobble revetment was installed at the location of the sand beach berm

97 and was designed such that its crest height was at the elevation of the $R_{2\%}$ runup level
 98 measured during Phase SB for the second water level increment to ensure significant
 99 overtopping as the water level was increased. The sand foreshore and dynamic revetment
 100 were then allowed to reshape under constant wave conditions over the remaining water
 101 level increments, with the test durations at each water level mirroring those in Phase SB (38
 102 hours of water level rise testing). Finally, higher energy storm waves were used at the end of
 103 the final water level increment to investigate revetment resilience to higher energy
 104 conditions.

105 The availability to researchers of large-scale measurements of nearshore hydro and
 106 morphodynamics at the spatio-temporal resolution achieved during DynaRev is very limited.
 107 Potential uses for the datasets obtained during the DynaRev test program are wide-ranging
 108 and include: the assessment of dynamic cobble berm revetment performance⁶, the
 109 investigation of nearshore processes such as the formation and dynamics of nearshore
 110 sandbars⁷, the response of sandy coasts to a rising sea level⁸, morphology change in the
 111 swash zone⁹, wave-by-wave sediment transport rates¹⁰, air entrainment in breaking waves⁷
 112 and the development of numerical models⁸.

113



114

115 **Figure 1 (a)** Schematic of flume setup showing primary instrument locations (see Table 1).
 116 The yellow shaded area represents the sand volume and the dark grey shaded area is the
 117 permanent 1:6 impermeable slope. The black solid and dashed horizontal lines indicate the
 118 minimum ($z_{wl} = 4.5\text{m}$) and maximum ($z_{wl} = 4.9\text{m}$) water levels. **(b)** Close up of the dynamic
 119 cobble berm revetment geometry after construction corresponding to the grey box in (a).
 120 The minimum water level used for revetment testing ($z_{wl} = 4.6\text{ m}$) is shown as a solid
 121 horizontal line and the dashed line indicates the maximum water level. The light grey region
 122 indicates the constructed dynamic revetment and the dot-dashed line shows the beach
 123 profile prior to revetment construction. **(c)** Photograph of the constructed dynamic
 124 revetment on the underlying sand beach. The yellow line indicates the initial line of the
 125 revetment crest.

126

127 **Methods**

128 In this section, the experimental facility and test program are described, followed by the
129 details of the instrumentation.

130 **Experimental Setup and Morphology**

131 The GWK large wave flume is 309 m long, 7 m deep and 5 m wide with a combined piston-
132 flap type wavemaker. A schematic of the experimental setup is shown in Figure 1. All
133 coordinates are given as the distance from the wave paddle rest position ($x = 0$ m), elevation
134 above the horizontal flume bed ($z = 0$ m) and across-flume distance from the centreline ($y = 0$
135 m). The flume was filled with fresh water from the Mittelland canal which runs adjacent to
136 the facility.

137 A large suite of instruments was deployed during the experiment and is detailed below. All
138 instruments were logged by PCs connected to a local area network with a shared timeserver
139 to ensure time-synchronisation. Table 1 lists all instruments and their locations within the
140 flume, and the primary instrument positions are shown in Figure 1 (noting that some
141 instruments were moved in response to water level increases and/or evolving beach
142 morphology).

143 Both phases of the experiment used an initially planar sand beach with a gradient of 1:15
144 which was placed on top of a permanent 1:6 asphalt slope with a minimum sand depth of 3.1
145 m beneath the active part of the profile (seaward of the maximum runoff limit, $x = 278$ m).
146 The beach was constructed using 1660 m³ of medium-coarse quartz sand ($D_{50} = 330$ μm , D_{90}
147 = 650 μm and $D_{10} = 200$ μm) from the GWK facility's material store. The sand had a density of
148 2650 kg/m³ and dry bulk density of 1680 kg/m³ giving a porosity of 0.37. A 25 m long layer of
149 sand with a thickness of 0.5 m was installed in front of the slope in order to provide an
150 additional supply of sediment. The toe of this layer was located at $x = 161$ m, the toe of the
151 beach slope at $x = 188.5$ m and the top of the slope was at $x = 283$ m, $z = 6.8$ m (Figure 1a).

152 After the first water level rise of Phase DR, a dynamic cobble berm revetment was
153 constructed on the modified sand beach profile. The revetment was composed of 9.375 m³
154 (15 tonnes) of well sorted rounded granite cobbles with characteristics $D_{max} = 90$ mm, $D_{min} =$
155 50 mm, $D_{50} = 63$ mm, $D_{85}/D_{15} = 1.32$, bulk density = 1600 kg/m³ and porosity = 0.41. The toe
156 of the revetment was located at $x = 256.8$ m, $z = 4.77$ m, with a 1:6 slope leading to the crest
157 at $x = 260.7$ m, $z = 5.42$ m. The overall height and width of the constructed revetment was
158 0.65 m and 7.3 m respectively. The revetment slope was selected based on guidance for
159 recharge of shingle beaches¹³ and the crest elevation was designed to be at the elevation of
160 the $R_{2\%}$ runoff level for the second water level increment measured during Phase SB using the
161 Lidar.

162 The top of the revetment extended horizontally from the crest until it intersected with the
163 sand beach at $x = 264.1$ m, $z = 5.42$ m. Note that due to the slope of the modified sand
164 profile approaching that of the designed revetment at the installation location, it was
165 necessary to dig out 7.2 m³ of sand to enable the designed cobble volume to be placed (see
166 Figure 1).

167 **Table 1:** Summary of the measurement instruments deployed during the experiment
 168 including: Instrument type, measurement purpose, measurement units and primary
 169 instrument locations noting that some instruments were moved during the experiment as
 170 described in the manuscript.

Abbrev.	Instrument	Purpose (measurement units)	x (m)	z (m)
WG1	Wave gauge	Array 1: Water surface elevation in the deep flume section, η (m)	50	-
WG2	Wave gauge		51.9	-
WG3	Wave gauge		55.2	-
WG4	Wave gauge		60	-
WG5	Wave gauge	Array 2: Water surface elevation in the deep flume section, η (m)	160	-
WG6	Wave gauge		161.9	-
WG7	Wave gauge		165.2	-
WG8	Wave gauge		170	-
ADV1	Nortek Vector	Flow velocity, u, v, w (ms^{-1}) – shoaling waves	180	2.5
ADV2	Nortek Vector	Flow velocity, u, v, w (ms^{-1}) – surf zone	235	3.67
ADV3	Nortek Vector		242	4.22
WGADV1	Wave gauge	Water surface elevation at ADV1 location, η (m)	180	2.5
PTADV2	Pressure transducer	Pressure at ADV2 location, P (kPa)	235	3.67
PTADV3	Pressure transducer	Pressure at ADV3 location, P (kPa)	242	4.22
PT3	Pressure transducer	Pressure between the surf zone/ bar processes instrument rigs, P (kPa)	231.7	4.13
LID1	SICK LMS511 2D Lidar	High spatio-temporal resolution water surface profile, η (m) – surf zone	230.04	11.76
LID2	SICK LMS511 2D Lidar		242.02	11.85
LID3	SICK LMS511 2D Lidar	Swash surface profile, η (m), Beach/revetment profile, z (m)	254.99	11.82
CAM	Vivotek IB9381-HT high resolution camera	Surf, Swash	Adjustable (276-280m)	11.8
MB	Reson 7125 Multibeam	Bubble cloud, Bathymetry, x, z (dB)	Adjustable	Adjustable
FARO	FARO Focus 3D (Lidar)	3D topography (m)	Adjustable	Adjustable
RFID	Instrumented cobbles	Cobble movement	97 cobbles placed at 3 depths along the revetment centreline	
Surf Zone Instrumentation				
Rigs were reset to maintain constant instrument elevations above the bed at the start of every test, thus all elevations are presented in cm relative to the local bed and given the notation h .				
Abbrev.	Instrument	Purpose (measurement units)	x (m)	h (cm)
PT1	Pressure transducer	Pressure, P (kPa)	226.5	45
OBS1	Optical backscatter sensor	Suspended sediment concentration, C (kg/m^3)		10
OBS2	Optical backscatter sensor			5
RPR1	Ripple Profiler	Bed profile, z (m)		76
EM1	Valeport Electromagnetic Current Meter	Flow velocity, u, v (ms^{-1})	233.5	5
EM2	Valeport Electromagnetic Current Meter			10
PT2	Pressure transducer	Pressure, P (kPa)		45
OBS3	Optical backscatter sensor	Suspended sediment concentration, C (kg/m^3)		10
OBS4	Optical backscatter sensor		5	
RPR2	Ripple Profiler	Bed profile, z (m)	75	
EM3	Valeport Electromagnetic Current Meter	Flow velocity, u, v (ms^{-1})	11	
EM4	Valeport Electromagnetic Current Meter		5.5	

171

172 **Test Program**

173 The experiment was divided into two phases corresponding to sand beach (Phase SB) and
 174 dynamic revetment (Phase DR) testing. Within each phase, the profile was monitored as it

175 evolved under wave forcing and increasing water level. Testing within each phase was
176 undertaken at 5 different water levels (0.1 m increments), and at each water level the
177 experiment was divided into “runs” of increasing duration as the rate of morphological
178 change reduced (133 runs in total). An overview of the test program is provided in Table 2
179 and the details of all runs are listed in the dataset associated with this paper. The initial case
180 for both phases was a 1:15 planar sand beach with a water level $z_{wl} = 4.5$ m and as previously
181 noted the beach profile was only reset between the two phases, thus all runs had a different
182 antecedent morphology corresponding to the beach profile the end of the preceding run.

183 ***Phase SB - Unmodified sand beach response***

184 Starting with an initially planar slope and a water level $z_{wl} = 4.5$ m, the beach was first
185 allowed to evolve naturally under constant wave forcing ($H_s = 0.8$ m, $T_p = 6.0$ s). The mean
186 water level in the flume was raised by a total of 0.4 m in steps of 0.1 m. Measurements were
187 undertaken for a period of 20 and 17 hours for the first ($z_{wl} = 4.5$ m) and final ($z_{wl} = 4.9$ m)
188 water levels, and for 7 hours at the intermediate levels. In total, this testing was divided into
189 63 runs with durations ranging from 20 minutes to 3 hours. Run names for this phase are
190 given as SB<WL increment>_<Run No.>, where water level (WL) increments are numbered 0
191 for the initial water level of 4.5 m to 4 for $z_{wl} = 4.9$ m and run numbering is started from 1 for
192 each WL increment.

193 Following the completion of the WL increments, “resilience testing” was completed to
194 investigate the short-term response of the beach to a range of different wave conditions
195 (“tests”) expected to produce both erosion and accretion. This testing was undertaken at
196 the highest water level ($z_{wl} = 4.9$ m). Each test was divided into 3 to 7 runs with durations
197 ranging from 20 to 60 minutes. These runs were labelled SBE for erosive cases and SBA for
198 cases expected to cause accretion, numbered according to test number and then run
199 number, e.g. SBE1_3 for erosive test 1, run 3.

200 ***Phase DR – Dynamic cobble berm revetment response***

201 Initially, a 1:15 planar sand beach was allowed to reshape naturally under constant wave
202 conditions ($H_s = 0.8$ m, $T_p = 6.0$ s) for 20 hours, repeating the first WL increment of Phase SB
203 ($z_{wl} = 4.5$ m) to provide a natural beach profile on which to construct the dynamic cobble
204 berm revetment. The cobble revetment was installed at the location of the sand beach berm
205 according to the configuration given in section 2.1. The revetment was designed such that it
206 would be overtopped significantly as the water-level rose. The sand foreshore and dynamic
207 revetment were then reshaped by waves (constant conditions; $H_s = 0.8$ m, $T_p = 6.0$ s) for the
208 remaining water level increments, with the test durations at each water level mirroring those
209 in Phase SB. Run names for this phase are given as DR<WL increment>_<Run No.>, where
210 WL increments and run numbers follow those for Phase SB.

211 After completion of the WL increments, “resilience testing” of the revetment under varying
212 wave conditions was undertaken at the highest water level, $z_{wl} = 4.9$ m. Each test was divided
213 into 2 to 4 runs with durations ranging from 20 to 60 minutes. These runs were labelled DRE
214 for erosive cases and DRR for cases expected to allow the revetment to recover, and
215 numbered as per the Phase SB resilience tests.

216 Finally, to investigate the effect of recharging the revetment, 2.5 m³ of additional cobbles,
 217 corresponding to a 0.2 m thick layer were placed on the front face of the revetment.
 218 Following this recharge, the response of the revetment to a range of different high energy,
 219 erosive wave cases was measured. These runs were labelled DRN and numbered using the
 220 same notation as the resilience tests.

221 **Table 2:** Overview of the test program. The times in the program when 3D Lidar scans and
 222 RFID surveys were completed are marked with an asterisk and dagger (+) respectively in the
 223 'Run Durations' column. A more detailed breakdown of the test program is given in the
 224 'DynaRev_TestProgram.xlsx' file provided in the dataset associated with this experiment.

WL increment/Test	Duration (hr)	H _s (m)	T _p (s)	Water level z _{wl} (m)	Number of Runs	Run Durations (minutes)
Phase SB - Morphological response of a sandy beach with a rising water level						
SB0	20	0.8	6	4.5	14	*20,20,20,30,30,60,60*,60,120,120,120,180,180,180
SB1	7	0.8	6	4.6	9	20,20,20,30,30,60,60,60,60,60
SB2	7	0.8	6	4.7	7	20,40,60,60,60,60,120*
SB3	7	0.8	6	4.8	7	20,40,60,60,60,60,120
SB4	17	0.8	6	4.9	11	20,40,60,60,60,60,120,120,120,180,180
Phase SB – Resilience testing at the maximum water level z_{wl} = 4.9 m						
SBE1	2	1	7	4.9	3	20,40,60
SBE2	4	1.2	8	4.9	5	20,40,60,60,60,60
SBA1	6	0.6	12	4.9	7	20,40,60,60,60,60,60*
Phase DR – Morphological response of a sandy beach with a dynamic revetment to a rising water level						
DR0	20	0.8	6	4.5	14	*20,20,20,30,30,60,60,60,120,120,120,180,180,180*
Dynamic revetment installation						
DR1	7	0.8	6	4.6	9	*+20,20,20,30,30,60,60,60,120†
DR2	7	0.8	6	4.7	7	20,40,60,60,60,60,120*†
DR3	7	0.8	6	4.8	7	20,40,60,60,60,60,120*†
DR4	17	0.8	6	4.9	11	20,40,60,60,60,60,120*†,120,120,180,180*†
Phase DR – Resilience testing at the maximum water level z_{wl} = 4.9 m						
DRE1	2	0.9	6	4.9	3	20,40,60†
DRE2	2	1	7	4.9	4	20,20,20,60†
DRE3	1	1	8	4.9	3	20,20,20
DRR1	2	0.8	6	4.9	2	60,60
Phase DR – Resilience testing with recharged revetment at the maximum water level z_{wl} = 4.9 m						
DRN1	2	0.8	6	4.9	2	60,60†
DRN2	0.66	1.0	8	4.9	2	20,20
DRN3	2	0.8	6	4.9	2	60,60
DRN4	0.66	1.0	9	4.9	2	20,20
DRN5	0.33	1.2	8	4.9	1	20
DRN6	1	0.8	6	4.9	1	60

225 **Wave conditions**

226 Wave paddle steering signals were generated according to the JONSWAP spectrum (using a
 227 peak enhancement coefficient of 3.3) specified using significant wave height, H_s and peak

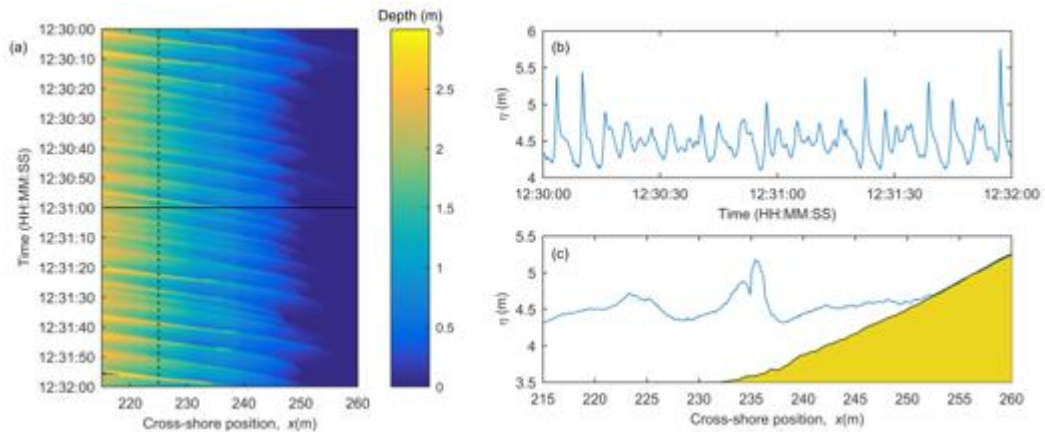
228 wave period T_p . For Phases SB and DR constant wave forcing was applied, $H_s = 0.8$ m and $T_p =$
229 6 s. This wave condition was chosen to be mildly erosive based on experience at the
230 BARDEX2 experiment³, which had a similar setup and according to criteria based on
231 dimensionless fall velocity¹⁵. For each of the five water levels used, a two-hour long wave
232 paddle signal was generated to produce an identical timeseries of waves at the wave paddle,
233 taking water depth into account. These two-hour signals were segmented to account for the
234 durations of the runs (20, 30, 40, 60, 120 and 180 minutes) to allow the same two-hour
235 signal to be repeated multiple times at each WL increment with interruptions for beach
236 profiling. Reflected waves as well as low frequency resonance were damped at the paddle
237 using an automatic reflection compensation.

238 For the resilience testing, erosive and accretionary wave conditions were specified primarily
239 based on dimensionless fall velocity criteria^{14,15,16}. The erosive cases were ordered such that
240 the wave energy and wave runup increased with each consecutive run. Note that the wave
241 cases used for the Phase DR resilience testing (DRE and DRR) were different to those used
242 during Phase SB because they were modified during the experiment to investigate the
243 observed relationship between wave period and revetment slope⁶.

244 **Wave measurements**

245 The incident and reflected wave fields were measured offshore of the beach using a pair of
246 combined surface-piercing resistance-capacitance wave gauge arrays, each comprising four
247 gauges. The seaward gauges in each array were located at $x = 50$ m and $x = 160$ m, with
248 spacings of 1.9 m, 3.3 m and 4.8 m between consecutive gauges. A further wave gauge was
249 located at $x = 180$ m and was co-located with a Nortek Vector acoustic Doppler velocimeter
250 (ADV) which was positioned to measure wave conditions at the toe of the sand beach slope.

251 Measurements of the time-varying water surface elevation throughout the surf and swash
252 zones were obtained using an array of three SICK LMS511 2D Lidar instruments mounted in
253 the flume roof at an elevation, $z = 11.8$ m and at cross-shore positions $x = 230, 242$ and 255
254 m. The sampling rate of all three scanners was 25 Hz with an angular resolution of 0.166° .
255 The dense spacing of the Lidars in the array ensured complete coverage of the surf and
256 swash zones ($x = 221.4$ m to $x = 275.8$ m) throughout the experiment, with at least 12 m of
257 overlap between the scanning regions of adjacent instruments. The use of Lidar arrays to
258 obtain wave data throughout the surf and swash zone has been successfully demonstrated¹⁷.
259 Typically, Lidar requires bubbles to be present on the water surface to ensure that the
260 incident laser light is scattered sufficiently to obtain a valid detection. During the experiment
261 described here, it was found that the instruments performed better than during previous
262 field deployments^{17,18,19}, with valid return signals even when levels of aeration were very low
263 or in some cases, non-existent. It is thought that this was due to the presence of fine
264 sediment in the water column which caused light to be scattered from the water surface.
265 Example wave data obtained using the Lidar array is shown in Figure 2.



266

267 **Figure 2:** Example wave measurements. **(a)** Timestack of water depth measured by the Lidar
 268 throughout the surf and swash zones. **(b)** Timeseries of water surface elevation at $x = 225\text{m}$
 269 as indicated by the vertical dashed line in (a). **(c)** Measured free-surface profile through the
 270 surf and swash zone at the time indicated by the horizontal solid line in (a). Note that the
 271 measurements capture the splash-up generated by a breaking wave at $x=235.5\text{ m}$.

272 Morphology measurements

273 The emergent and submerged beach profile, between $x = 183\text{ m}$ and $x = 270\text{ m}$ was
 274 measured at the end of each run using a mechanical roller attached to the overhead trolley
 275 which ran along the centre of the flume. Figure 3a shows an example profile measurement.

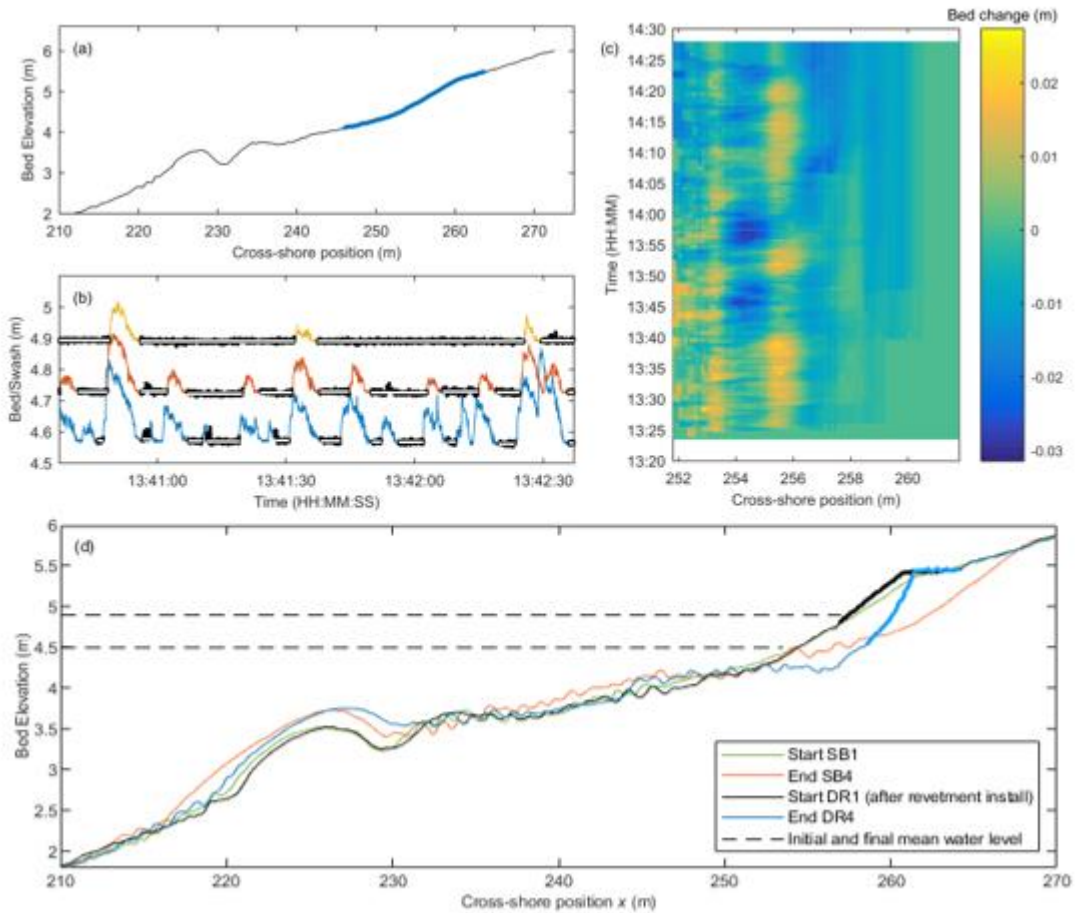
276 A Reson SeaBat 7125 multibeam echo-sounder was deployed to obtain pilot measurements
 277 of the bubble clouds generated by wave breaking¹¹ and non-intrusive, regular measurements
 278 of the submerged beach profile. The echo-sounder was mounted on a vertical arm fixed to
 279 the overhead trolley of the mechanical profiler. The receiver was oriented in the vertical
 280 plane and aligned centrally along the length of the flume. A range of different cross-shore
 281 locations, depths and angles were tested to optimise data collection leading to a primary
 282 deployment position of $x = 223.71$, $z = 3.8\text{m}$ and an angle of 30° above the horizontal. The
 283 instrument has a 128° opening angle 0.54 beam divergence angle, operates at a frequency of
 284 400 kHz and measurements in units of dB were collected at 1 ping per second. Note that the
 285 shallow depths and presence of bubble clouds during wave sequences make regular
 286 detection of the changing bed difficult using conventional processing methods, however new
 287 algorithms which make use of the double acoustic reflection from the water surface to the
 288 bed and back to the receiver are being developed and will be reported in future works. Due
 289 to the pilot nature of this deployment, the multiple instrument positions and orientations
 290 used, the size of the dataset and the large quantity of noisy data, the multibeam dataset is
 291 not provided in the downloadable dataset.

292 Wave-by-wave measurements of the changing beach face profile were obtained using the
 293 landward-most Lidar located at $x = 255\text{ m}$. Lidar detects the uppermost surface at each scan
 294 position within the swash zone – either swash surface (when submerged) or the emergent
 295 bed (between swash events). By separating the “swash” and “bed” signals within the Lidar
 296 dataset using a variance-based approach²⁰ (see Figure 3b) it is possible to obtain the beach
 297 profile landward of the swash rundown position between every swash event (Figure 3c). The

298 quoted error range for the Lidar is ± 6 mm, however testing has demonstrated that for a
299 stationary sand or cobble bed, this range is reduced to approximately ± 0.95 mm.

300 Measurements of the entire three-dimensional bathymetry were obtained at irregular
301 intervals when the flume was drained using a FARO Focus 3D terrestrial laser scanner. A
302 total of 11 surveys of this type were completed throughout the duration of the experiment.

303



304

305 **Figure 3:** Example morphology data. **(a)** An example beach profile as measured by the
306 mechanical profiler (black) and the swash zone profile obtained from the Lidar data (blue).
307 **(b)** Separation of bed (black dots) and swash data at $x = 253.8$ m (blue), $x = 255.3$ m (red) and
308 $x = 256.8$ m (orange) for an example section of data. The mean bed elevation between each
309 swash event is shown in white. **(c)** Bed elevation change relative to the initial profile in the
310 swash zone at the wave-by-wave timescale. **(d)** Beach profile data showing the evolution of
311 the sand beach and dynamic revetment modified from Bayle et al.⁶. The revetment surface is
312 marked with a thicker line.

313 Surf Zone/ Sandbar Measurements

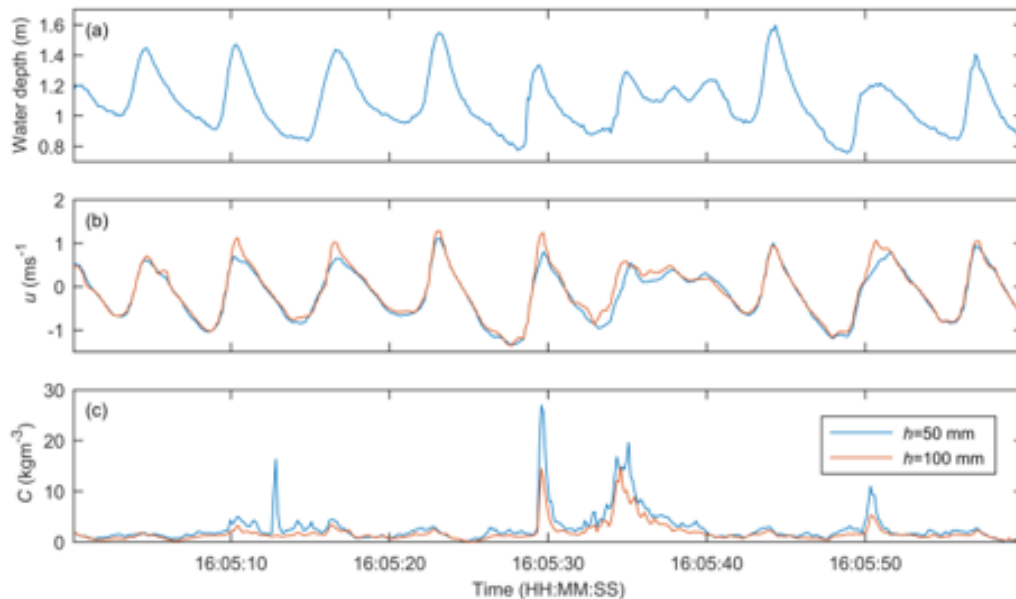
314 Two measurement rigs were installed immediately landward and seaward of the predicted
315 sandbar location and each housed an array of instrumentation designed to measure
316 hydrodynamics, sediment transport and morphological change during bar formation and
317 migration. The main instrument mounting bars for these rigs were located at $x = 226.5$ and
318 233.5 m. Each of the measurement rigs was fixed to the walls on a mechanism such that

319 they could be lifted and lowered manually to the bed after each run to ensure that all
320 instruments remained a constant height above the evolving bed (see Table 1).

321 Each rig was equipped with the following instruments which were sampled at 8 Hz: 2 optical
322 backscatter sensors (OBS) mounted at 5 and 10 cm from the bed, two electromagnetic
323 current meters (EMCM) at elevations of 5 and 10 cm above the bed and a pressure
324 transducer (PT) mounted 45 cm above the bed. The error ranges of the EMCMs and PTs are
325 approximately $\pm 0.015 \text{ ms}^{-1}$ and $\pm 0.6 \text{ Pa}$ respectively. Finally, a ripple profile scanner (RPS)
326 was mounted 75 cm above the bed to obtain local bed profile measurements along a 0.9 m
327 transect. The RPS on each rig was sampled alternately for one minute to avoid crosstalk
328 between instruments.

329 In addition to the two rigs, two Nortek ADVs were located at $x = 235$ and 242 m , maintained
330 at a height 15 cm above the bed and sampled at 25 Hz. Each ADV was co-located with a
331 pressure transducer and an additional standalone pressure transducer was installed at $x =$
332 231.7 m , $z = 4.13 \text{ m}$. The error range for the ADVs for the velocities measured is
333 approximately $\pm 0.01 \text{ ms}^{-1}$.

334 Note that the two surf zone rigs described here were present for the entirety of Phase SB
335 and the first 20 hours of the Phase DR testing. The instruments and scaffold rigs were
336 removed during installation of the dynamic cobble berm revetment to avoid the risk of
337 damage due to impact from stray cobbles from the revetment. Example post-processed data
338 from the seaward surf zone rig is presented in Figure 4.



339

340 **Figure 4:** Timeseries data from surf zone rig 1, $x = 226.5 \text{ m}$. **(a)** Water depth derived from
341 pressure transducer data, **(b)** cross-shore flow velocity measured 5 cm (blue) and 10 cm (red)
342 above the bed using EMCMs, and **(c)** suspended sediment concentrations 5 cm (blue) and 10
343 cm (red) above the bed measured using OBS.

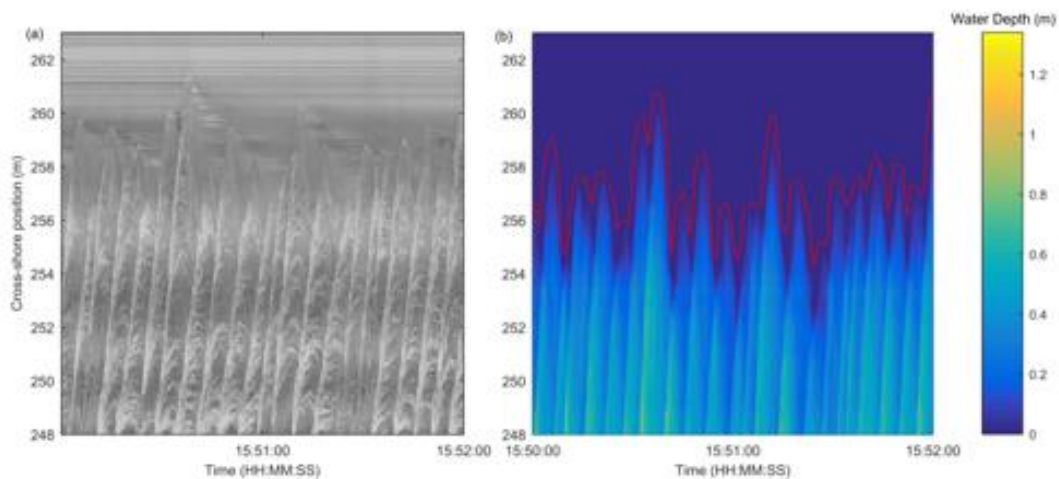
344 Swash zone measurements

345 The swash zone was monitored by a high definition IP camera (Vivotek IB9381-HT) which was
346 used in RGB mode, the frame rate was 10 fps with a resolution of 2560x1920 px. The camera

347 was mounted in the flume roof at $z = 11.8$ m landward of the runup limit, facing the wave
348 paddle. The cross-shore position of the camera varied with the water level in the range $x =$
349 267 m to 280 m. A series of ground control points (GCPs) were positioned within the camera
350 field of view to enable generation of rectified timestack images. The position of these GCPs
351 was surveyed using the FARO Focus 3D terrestrial laser scanner.

352 The timestack images of swash flow are complimented by the data from the most landward
353 Lidar which monitored flow depths and bed elevations within the swash zone. Separation of
354 the “bed” and “swash” using variance criteria²⁰ as described above enables not only
355 extraction of wave-by-wave bed elevations, but also estimates of the shoreline timeseries
356 and depth-averaged flow velocity²¹ and capture of the bore collapse process¹⁹. Example
357 swash zone measurements are presented in Figure 5.

358



359

360 **Figure 5:** Example swash data. **(a)** Video timestack extracted from the high definition video.
361 **(b)** Timestack of water depth extracted from the Lidar data with the timeseries of shoreline
362 position added in red.

363 Instrumented Cobbles

364 The movement of individual cobbles within the dynamic revetment was monitored using an
365 RFID tracking system similar to that previously used in field experiments²². The RFID system
366 consists of three components: Passive Integrated Transponder (PIT) tags, the module reader
367 and the antenna.

368 Texas Instruments TRPGR30ATGA PIT tags with a unique identification number and a
369 detection range of 0.6 m were installed in 97 cobbles. The tags were placed inside 5 mm
370 diameter holes drilled into the short axis of the cobbles and sealed using epoxy glue.
371 Following PIT installation, the cobbles were washed, dried and painted in 3 different colours:
372 20 cobbles were painted pink and placed on the bottom layer of the revetment (at the sand
373 interface) during its construction; 30 cobbles were painted orange and placed 20 cm above
374 the bottom of the revetment (mid layer); 47 cobbles were painted green and placed at the
375 toe and on the top layer of the revetment. All cobbles were placed along the centre line of
376 the revetment in groups of 3 cobbles at 0.4 m cross-shore intervals. An additional 7 cobbles

377 were initially placed at the revetment toe. Finally, the crest line of the revetment was
 378 painted yellow to enable modification of the crest by waves to be easily observed (Figure 1c).
 379 Further details of the instrumented cobble placement are provided by Bayle et al.⁶ and the
 380 'DynaRev_RFID.xlsx' spreadsheet provided in the dataset associated with this paper details
 381 the initial cobble positions and locations in each RFID survey.

382 The RFID reader used here was a Texas Instrument Series 2000 RI-STU-251B which transmits
 383 a radio frequency of 130.2 kHz and was connected to a logging computer via an RS232 serial
 384 connection. A 120 dB beeper was used to provide an audible beep when a PIT was detected.
 385 A Texas Instrument Ri-ANT-G02E antenna was connected to the module reader. The antenna
 386 measured 20 cm by 20 cm and was attached to a telescopic pole (up to 5 m long) to allow
 387 cobble detection from the side of the flume, avoiding the need for the operator to walk on,
 388 and potentially damage the revetment. Instrumented cobble surveys were completed at the
 389 end of each water level increment and day of testing during Phase DR by passing the
 390 antenna over the revetment surface in a systematic manner. The identification number and
 391 cross-shore position of each detected cobble was recorded for each survey.

392 Data Records

393 The data detailed in this paper is available for download from DOI
 394 10.5281/zenodo.3889796²³. Additional metadata is provided within each *.mat file detailing
 395 how the data from each instrument is stored. Note also that all raw, unprocessed data is
 396 available at DOI 10.5281/zenodo.3855650.

397 **Table 3:** Data files associated with the DynaRev experiment available from DOI
 398 10.5281/zenodo.3889796.

Filename	Data description	Instruments (ref. Table 1)
DynaRev_TestProgram.xlsx	Complete list of test cases	-
DynaRev_Profiles.mat	Beach profiles measured after each run (x,z)	Mechanical profiler
DynaRev_Paddle_Files.zip	Wave paddle driver files in ascii format	Wave paddle
DynaRev_DAQ.mat	Timeseries data collected by the central data acquisition system: <ul style="list-style-type: none"> • Wave gauges - surface elevation, η (m) • ADVs – flow velocity, u,v,w (ms^{-1}) • PTs – pressure, P (kPa) • Paddle stroke (m) 	WG1 to 8, WGADV1 ADV1, ADV2, ADV3 PTADV2, PTADV3 Measured wave paddle stroke
DynaRev_SurfZone.mat	Timeseries data from the surf zone rigs: <ul style="list-style-type: none"> • PTs – pressure, P (kPa) • EMCMS – flow velocity, u,v (ms^{-1}) • OBS – sediment concentration, C (gL^{-1}) 	PT1, PT2, PT3 OBS1 to OBS 4 EM1 to EM4
DynaRev_Lidar_<Phase><WL increment>-<Run No.>.mat	Timeseries x, z data from the combined Lidar array in .mat format. The data for each run is stored in a separate file, e.g. "DynaRev_Lidar_SB1-5.mat" contains the data for Phase SB, WL 1 ($z_{wl} = 4.6$ m), Run 1.	LID1, LID2, LID3
DynaRev_TimeStack.mat	Image timestack of swash zone	CAM
DynaRev_RFID.xlsx	Table containing instrumented cobble positions	RFID
DynaRev_3Dscans.zip	Point cloud data (x,y,z (m)) from 11 3D Lidar scans of the morphology in ".xyz" format	FARO
DynaRev_Lib	Scripts for post-processing raw instrument data	

399

400 **Technical Validation**

401 All data was collected using well-established coastal field and/or laboratory techniques using
402 commercially available instrumentation. Post-processing was undertaken to remove outliers
403 and convert spatial data to the x, y, z coordinate system defined above.

404 The profiler system provides the beach profile data directly in the local coordinate system ($x,$
405 z). A visual check was completed directly after each profile to ensure no obvious
406 measurement errors. Where errors were detected, the profile was repeated. The elevation
407 data was interpolated onto a 0.025 m cross-shore grid.

408 The output from each Lidar provides the distance to the nearest target for every angle within
409 each 2D scan at 25 Hz. This data was converted to local Cartesian coordinates (x, z) based on
410 the position and orientation of each Lidar within the flume and interpolated onto a 0.1 m
411 cross-shore grid. Outliers were only obtained where an object or person was positioned
412 within the Lidar scan and these were removed manually. The exact location and orientation
413 of the Lidar array was confirmed through comparison with the mechanical beach profiler
414 data when no waves were running (see Figure 3a). A RMSE smaller than 0.014 m was
415 obtained.

416 Data from the wave gauges, ADVs, PTADV1 and PTADV2 (see Table 1) were sampled by the
417 central GWK data acquisition system at 25 Hz. All wave gauges were calibrated at regular
418 intervals throughout the experiment using a standard procedure. For each calibration, the
419 water level was lowered from 5 m to 0.5 m in increments of 0.3 m and the voltage from all
420 wave gauges at each water level was recorded for 180 s to create a calibration function
421 relating water level to voltage. Wave gauge data was provided by the GWK system as a
422 timeseries of water surface elevation in metres relative to the mean water level. ADV data
423 was provided as u, v, w velocities (ms^{-1}) and the pressure data were corrected for
424 atmospheric pressure and provided in kPa.

425 In the surf zone, PTs were sampled at 8 Hz, corrected for atmospheric pressure and provided
426 in kPa. EMCM data was sampled directly as u, v velocities at 8 Hz, no further post-processing
427 was undertaken. The time-varying free surface elevations obtained from the Lidar data were
428 compared with point measurements from pressure transducers PT1, PT2 and PT3 and wave
429 gauge WGADV1 (see Table 1). For all runs the signals matched closely with zero lag.

430 All optical backscatter sensors were calibrated after the experiment to provide sediment
431 concentration (gL^{-1}) by applying the method of Betteridge et al.²⁴ using sand from DynaRev in
432 a specially constructed sediment tower at the University of Plymouth.

433 Camera timestacks were processed by extracting a line of pixels along the flume centreline
434 and rectified using surveyed ground control points within the camera field of view.

435 **Code Availability**

436 All code provided in DynaRev_Lib is written in MATLAB (R2019b). This folder contains the
437 scripts used to process the raw data in order to obtain the post-processed data provided
438 within the repository.

439 The 3D Lidar point clouds described in Table 3 are provided in “.xyz” format which can be
440 opened using the open source CloudCompare software package. The filename for each scan
441 includes the date collected and the run after which the scan was completed, e.g.
442 20170918_DR2_7.xyz was completed after Run DR2-7 on 18th September, 2017. A table
443 providing the timings and notes about each scan is included within the DynaRev_3Dscans
444 data record.

445 **References**

- 446 1. Almeida, L.P., Masselink, G., McCall, R. & Russell, P.E. Storm overwash of a gravel barrier:
447 Field measurements and XBeach-G modelling. *Coast. Eng.* **120**, 22-35 (2017).
448
- 449 2. Briganti, R., Dodd, N., Incelli, G. & Kikkert, G. Numerical modelling of the flow and bed
450 evolution of a single bore-driven swash event on a coarse sand beach. *Coast. Eng.* **142**, 62-76
451 (2018).
452
- 453 3. Masselink, G. *et al.* Large-scale Barrier Dynamics Experiment II (BARDEX II): Experimental
454 design, instrumentation, test program, and data set, *Coast. Eng.* **113**, 3-18 (2016).
455
- 456 4. Eichentopf, S., van der Zanden, J., Cáceres, I., Baldock, T.E. & Alsina, J.M. Influence of
457 storm sequencing on breaker bar and shoreline evolution in large-scale experiments. *Coast.*
458 *Eng.* **157**, 103659 (2020).
459
- 460 5. Allan, J.C., & Komar, P. Environmentally compatible berm and artificial dune for shore
461 protection. *Shore and Beach* **721**, 9-16 (2004).
462
- 463 6. Bayle, P.M. *et al.* Performance of a dynamic cobble berm revetment for coastal protection,
464 *Coast. Eng.*, **159**, 103712 (2020).
465
- 466 7. Price, T.D., Ruessink, B.G. & Castelle, B. Morphological coupling in multiple sandbar
467 systems - a review, *Earth Surf. Dyn.* **2**, 309-321 (2014).
468
- 469 8. Ranasinghe, R., Callaghan, D. & Stive, M. Estimating coastal recession due to sea level rise:
470 Beyond the Bruun rule, *Clim. Change.* **110**, 561-574 (2012).
471
- 472 9. Chardón-Maldonado, P., Pintado-Patiño, J.C. & Puleo, J.A. Advances in swash-zone
473 research: Small-scale hydrodynamic and sediment transport processes, *Coast Eng.* **115**, 8-25
474 (2016).
475
- 476 10. Blenkinsopp, C.E., Turner, I.L., Masselink, G. & Russell, P.E. Swash zone sediment fluxes:
477 Field observations, *Coast. Eng.* **58**, 28-44 (2011).
478
- 479 11. Bryan, O., Bayle, P.M., Blenkinsopp, C.E. & Hunter, A.J. Breaking wave imaging using lidar
480 and sonar. *IEEE J. Oceanic Eng.* **45**, 1-11 (2019).
481
- 482 12. McCall, R., Rijper, R.H. & Blenkinsopp, C.E. Towards the development of a morphological
483 model for composite sand-gravel beaches. In *Proc. 9th International Conference on Coastal*
484 *Sediments* (Eds. Wang, P., Rosati, J.D. & Vallee, M.) 1889-1900 (World Scientific, 2019).
485
- 486 13. Powell, K.A. *Dissimilar Sediments - Model tests of replenished beaches using widely*
487 *graded sediments*. Technical Report SR350 (HR Wallingford, 1993).
488

- 489 14. Hattori, M. & Kawamata, R. Onshore-Offshore transport and beach change. *Coast. Eng.*
490 **72**, 1175-1193 (1980).
491
- 492 15. Dean, R.G. Heuristic model of sand transport in the surf zone, In *Proc. 1st Australian*
493 *Conference on Coastal Engineering* 208-214 (Institution of Engineers, Australia, 1973).
494
- 495 16. Dalrymple, R.A. & Thompson W. Study of equilibrium beach profiles. In *Proc. 15th*
496 *International Conference on Coastal Engineering* 1277-1296 (ASCE, 1976).
497
- 498 17. Martins, K., Blenkinsopp, C.E., Power, H.E., Bruder, B., Puleo, J.A. & Bergsma, E.W.J. High
499 resolution monitoring of wave transformation in the surf zone using a LiDAR scanner array,
500 *Coast. Eng.* **128**, 37-43 (2017).
- 501 18. Puleo, J. A. *et al.* A Comprehensive Field Study of Swash-zone Processes, Part 1:
502 Experimental Design With Examples of Hydrodynamic and Sediment Transport
503 Measurements. *J. Waterw. Port Coast.* **140**, 14-28 (2013).
- 504 19. Bergsma, E.W.J., Blenkinsopp, C.E., Martins, K., Almar, R. & Almeida, L.P. Bore collapse
505 and wave run-up on a sandy beach. *Cont. Shelf Res.* **174**, 132-139 (2019).
506
- 507 20. Almeida, L.P., Masselink, G., Russell, P.E. & Davidson, M.A. Observations of gravel beach
508 dynamics during high energy wave conditions using a laser scanner. *Geomorph.* **228**, 15-27
509 (2015).
510
- 511 21. Blenkinsopp, C.E., Turner, I.L., Masselink, G. & Russell, P.E. Validation of volume
512 continuity method for estimation of cross-shore swash flow velocity, *Coast. Eng.* **57**, 953-958
513 (2010).
514
- 515 22. Allan, J. C., Hart, R., & Tranquili, J. V. The use of passive integrated transponder (pit) tags
516 to trace cobble transport in a mixed sand-and-gravel beach on the high-energy Oregon coast,
517 USA. *Mar. Geol.* **232**, 63-86 (2006).
518
- 519 23. Schimmels, S., Blenkinsopp, C. DynaRev - Dynamic Coastal Protection: Resilience of
520 Dynamic Revetments Under Sea Level Rise. *Zenodo* <https://doi.org/10.5281/zenodo.3855650>
521 (2020).
522
- 523 24. Betteridge, K.F.E., Thorne, P.D. & Cooke, R.D. Calibrating multi-frequency acoustic
524 backscatter systems for studying near-bed suspended sediment transport processes. *Cont.*
525 *Shelf. Res.* **28**, 227-235 (2007).
526

527 **Acknowledgements**

528 This project has received funding from the European Union's Horizon 2020 research and
529 innovation programme under grant agreement No 654110, HYDRALAB+. P. Bayle and G.
530 Hennessey are supported by a PhD scholarship through the EPSRC CDT in Water Informatics:
531 Science & Engineering (WISE). A. Hunter and O. Bryan were supported by a University of
532 Bath Alumni Fund grant. T. Baldock acknowledges support from the Australian Research
533 Council through Discovery grant DP140101302. R. McCall and H. Rijper acknowledge funding
534 provided by the "Hydro- and morphodynamics during extreme events" Deltares Strategic
535 Research Program. The authors would like to thank Aaron Barrett and Jak McCarroll for their
536 help with decommissioning the experiment and all staff at the GWK facility for their
537 assistance before, during and after the DynaRev experiment.

538

539 **Author contributions**

540 C.E.B. conceived the project with input from D.C., G.M., I.L.T, T.E.B, R.M. and A.R. P.M.B. and
541 C.E.B. did the primary experiment design and managed the experiment logistics, further
542 experiment design input was provided by D.C., G.M., I.L.T, T.E.B and A.H. P.M.B. led the
543 experimental team with all authors providing assistance at various stages during the
544 experiment including: setting up equipment, logging data, undertaking manual investigation
545 and decommissioning. S.S. and M.K. provided the primary in-house planning and experiment
546 assistance.

547

548 **Competing interests**

549 The authors declare no competing interests.

550

551

552